

Yu. Stadnyk<sup>1</sup>, V.A. Romaka<sup>2</sup>, A. Horyn<sup>1</sup>, L. Romaka<sup>1</sup>, V. Krayovskyy<sup>2</sup>,  
I. Romaniv<sup>1</sup>, M. Rokomanuk<sup>2</sup>

## Investigation of $Ti_{1-x}Mo_xCoSb$ Semiconducting Solid Solution

<sup>1</sup>Ivan Franko National University of Lviv, Lviv, Ukraine, e-mail: stadnykyu@gmail.com

<sup>2</sup>National University "Lvivska Politechnika", Lviv, Ukraine, vromaka@lp.edu.ua

The effect of doping of the TiCoSb compound (MgAgAs structure type) by Mo atoms on the features of the structural characteristics and behavior of the electrokinetic, energetic and magnetic properties of the  $Ti_{1-x}Mo_xCoSb$  semiconducting solid solution ( $x = 0 - 0.06$ ) in the temperature interval 80 - 400 K was studied. It was shown that including of Mo atoms ( $r_{Mo} = 0.140$  nm) in the TiCoSb structure by substitution of Ti atoms ( $r_{Ti} = 0.146$  nm) in 4a position is accompanied with non-monotonous variation of the lattice parameter values  $a(x)$ , indicating unpredictable structural changes. Based on analysis of the variation of the electric resistivity values, thermopower coefficient, magnetic susceptibility and energetic characteristics, it was concluded that simultaneous generation in the crystal of the structural defects of the donor and acceptor nature (donor-acceptor pairs), which generate corresponding energy levels in the band gap of semiconductor and determine its electrical conductivity.

**Keywords:** solid solution, electrical conductivity, thermopower coefficient, Fermi level.

Received 15.10.2019; accepted for publication 15.03.2020.

### Introduction

A semiconductive solid solution based on the TiCoSb semi-Heusler phase obtained by substitution of the Ti atoms ( $3d^24s^2$ ) at the 4a position by the Mo atoms ( $4d^55s^1$ ) was investigated in order to expand the number of materials with high efficiency of thermal energy conversion into electrical. At first, the task was to determine the formation of this solid solution, its homogeneity range, and what transformation of its crystal structure occurs. After all, it is necessary to take into account that Ti is located in IV group of the Periodic Table of chemical elements, and Mo is in VI group. In other words, we were aimed to synthesize a solid solution, replacing atoms in 4a site with a large difference in electronegativity.

Another fact is that an energy advantage for the formation of the TiCoSb compound [1-3] is the presence of the structural defects as vacancies in positions of Ti and Co atoms, which corresponds to the compound formula  $(Ti_{0.992})(Co_{0.986})Sb$ . The presence of vacancies in the positions of Ti and Co atoms, the wave functions of

which form a conduction band, is equivalent to the generation of vacancies as structural defects of acceptor nature. In this case, the Fermi level  $\varepsilon_F$  is located within the band gap  $\varepsilon_g$  in the formed impurity acceptor band  $\varepsilon_A$ . This location of the Fermi level  $\varepsilon_F$  indicates the hole type of conductivity of the semiconductive material.

During investigation of the  $Ti_{1-x}V_xCoSb$  solid solution [4-6], obtained due to substitution of Ti atoms in position 4a by V atoms, which is located in V group of the Periodic Table of chemical elements, it was established that impurity V atoms change the occupancy degree of crystallographic positions of Co and Ti(V) atoms in the unit cell. It was found that the introduction of V atoms into the structure of the TiCoSb compound results in the simultaneous generation of structural defects of the acceptor and donor nature, and their concentration varies according to different laws.

These are the initial conditions for the study of the  $Ti_{1-x}Mo_xCoSb$  solid solution.

## I. Experimental details

The samples of the  $\text{Ti}_{1-x}\text{Mo}_x\text{CoSb}$  solid solution were synthesized by direct arc-melting of the constituent elements (titanium, molybdenum, cobalt, and antimony with nominal purity above 99.99 wt. %) in electric arc-furnace under inert atmosphere. Then the alloys were annealed at 1073 K for 720 hours and subsequently quenched in ice water. X-ray phase analysis was performed using X-ray powder diffraction of the synthesized samples (diffractometer Huber Image Plate with  $\text{CoK}_\alpha$  radiation). The calculation of the crystallographic parameters was performed using the Fullprof Suite program package [7]. Chemical and phase compositions of the samples were examined by electron probe microanalysis (EPMA) (scanning electron microscope REMMA 102-02). The Green's function method (Coringa-Kohn-Rostoker method (KKR)) in Coherent Potential Approximation (CPA) and Local Density Approximation (LDA) was used to model the electronic structure [8]. For calculations by KKR method the licensed software AkaiKKR and SPR-KKR with LDA approximation for the exchange-correlation potential with Moruzzi-Janak-Williams (MJW) parameterization was used [9]. 1000  $k$ -points of the Brillouin zone were used for modeling of energy characteristics by DOS calculation. The width of the energy window was 22 eV and was chosen to capture all semi-core states of the  $p$ -elements. Full Potential (FP) with representing of the plane waves was used for calculations by Linear Muffin-Tin Orbital (LMTO) method. LDA approximation with MJW parameterization was also used as the exchange-correlation potential. Accuracy of the Fermi level  $\varepsilon_F$  position was equal to  $\pm 6$  meV. The temperature and concentration dependences of the electrical resistivity ( $\rho$ ), thermopower coefficient ( $\alpha$ ) (in relation to copper) were measured at temperatures  $T = 80 - 400$  K. The measurements of the magnetic susceptibility of the  $\text{Ti}_{1-x}\text{Mo}_x\text{CoSb}$  samples ( $x = 0.01 - 0.06$ ) were performed by Faraday method at room temperature.

## II. Study of the crystallographic characteristics of $\text{Ti}_{1-x}\text{Mo}_x\text{CoSb}$

According to the performed phase analysis, the samples of the  $\text{Ti}_{1-x}\text{Mo}_x\text{CoSb}$  solid solution belong to the MgAgAs structure type [10] and contain no traces of other phases (Fig. 1a). Microprobe analysis of the atom concentration on the surface of the  $\text{Ti}_{1-x}\text{Mo}_x\text{CoSb}$  samples showed their correspondence with the initial composition. Since the atomic radii of Ti ( $r_{\text{Ti}} = 0.146$  nm) and Mo ( $r_{\text{Mo}} = 0.140$  nm) are close, a slight decrease of the lattice parameter  $a(x)$  for  $\text{Ti}_{1-x}\text{Mo}_x\text{CoSb}$  was expected. However, the structural studies of  $\text{Ti}_{1-x}\text{Mo}_x\text{CoSb}$  revealed the complex behavior of the lattice parameter  $a(x)$  (Fig. 1b). Such behavior of  $a(x)$  for  $\text{Ti}_{1-x}\text{Mo}_x\text{CoSb}$  was unexpected. The crystal structure refinements due to low impurity content, the concentration of which is far beyond the precision of the device, did not allow to determine the way of Mo atoms introduction in the TiCoSb compound: whether the ordering of the structure occurs and the atoms occupy their proper positions, or simultaneously the impurity atoms occupy different crystallographic positions, and the structure remains disordered.

The obtained experimental result indicated that changes occurred in the crystal structure which generated the structural defects, and the behavior of the lattice parameter  $a(x)$  of  $\text{Ti}_{1-x}\text{Mo}_x\text{CoSb}$  is only an illustration of these changes. Our task is to identify such changes and to understand the transformation processes of the  $\text{Ti}_{1-x}\text{Mo}_x\text{CoSb}$  structure, which will allow us to correctly model the energetic and electrokinetic characteristics of semiconducting solid solution.

*A priori*, only from character of the lattice parameter  $a(x)$  behavior of  $\text{Ti}_{1-x}\text{Mo}_x\text{CoSb}$  it may seem that the small variation of  $a(x)$  values at  $x > 0.03$  indicates absence of Mo atom solubility (the limit of substitutional solid solution). However, if it takes into account the insignificant difference between atomic radii of Ti and Mo and substitution just in  $4a$  position of Ti atoms, then the argument of the lack solubility at  $x > 0.03$  concentration is unlikely.

On the other hand, if it takes into account structural

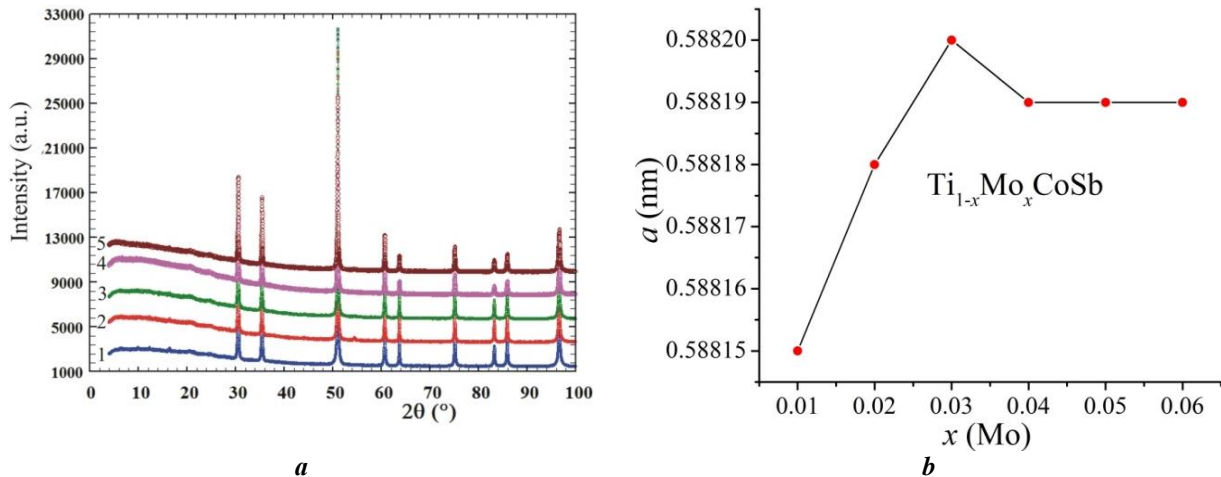


**Fig. 1.** Powder diffraction patterns of the  $\text{Ti}_{1-x}\text{Mo}_x\text{CoSb}$  samples: 1-  $x = 0.01$ , 2-  $x = 0.02$ , 3-  $x = 0.03$ , 4-  $x = 0.04$ , 5-  $x = 0.06$  (a) and variation of the lattice parameter  $a(x)$  (b).

studies of  $\text{TiCoSb}$  compound [1-3], which contains vacancies in the positions of Ti and Co atoms, a number of interesting questions arise upon the introduction of Mo atoms into the  $\text{TiCoSb}$  structure: whether impurity Mo atoms occupy the vacancies in  $4a$  position, or replace Ti atoms in this position? If Mo atoms occupy the vacancies in  $4a$  position or substitute Ti atoms in this position, then in both cases the structural defects of the donor nature were generated in the  $\text{Ti}_{1-x}\text{Mo}_x\text{CoSb}$  structure (higher number of  $d$ -electrons in Mo atom ( $4d^55s^1$ ) than in Ti atom ( $3d^24s^2$ )). In this case the impurity donor level (band)  $\varepsilon_D^2$  is formed in band gap near the conduction band  $\varepsilon_C$ .

If impurity Mo atoms occupy the vacancies in  $4c$  position of Co atoms, then the structural defects of the donor nature are also generated in the crystal. However, if Co atoms ( $3d^74s^2$ ) are substituted by Mo atoms, then the structural defects of acceptor nature are generated (the Mo atom contains less  $d$ -electrons than the Co atom), which create the impurity acceptor level (band)  $\varepsilon_A$  in the band gap. It's worth to note that this is practically unique method of acceptor generation in  $\text{Ti}_{1-x}\text{Mo}_x\text{CoSb}$ .

### III. Modeling of electronic structure and characteristics of $\text{Ti}_{1-x}\text{Mo}_x\text{CoSb}$

To predict the behavior of Fermi energy  $\varepsilon_F$ , band gap  $\varepsilon_g$ , electrokinetic characteristics of  $\text{Ti}_{1-x}\text{Mo}_x\text{CoSb}$  the calculation of the density of electronic states (DOS) (Fig. 2) was performed for ordered variant of its structure, in which the substitution of Ti atoms in  $4a$  position by Mo atoms takes place. Since in the  $\text{TiCoSb}$  at low temperatures the Fermi level  $\varepsilon_F$  is located near the valence band  $\varepsilon_V$ , then at the smallest concentration of Mo donor impurity the Fermi level  $\varepsilon_F$  of  $\text{Ti}_{1-x}\text{Mo}_x\text{CoSb}$  begins to drift to the conduction band  $\varepsilon_C$ , which be crossed at  $x \approx 0.03$ . In this case, the insulator-metal transition of conductivity (Anderson transition [6]) occurs, and electrons will be the main charge carriers. Such behavior of the Fermi level  $\varepsilon_F$  of  $\text{Ti}_{1-x}\text{Mo}_x\text{CoSb}$  is logical since donors are generated in the semiconductor under these conditions.

The calculation of the distribution of electronic states density DOS allows to simulate the behavior of the electric resistivity  $\rho(x, T)$ , thermopower coefficient  $\alpha(x, T)$ , thermal conductivity coefficient  $\kappa(x, T)$ , etc. As an example, the results of the modeling of thermopower coefficient  $\alpha(x, T)$  behavior for  $\text{Ti}_{1-x}\text{Mo}_x\text{CoSb}$  using equation (1) [11] are presented in Fig. 3a:

$$\alpha = \frac{2\pi^2 k^2 T}{3e} \left( \frac{d}{d\varepsilon} \ln g(\varepsilon_F) \right), \quad (1)$$

where  $g(\varepsilon_F)$  is density of states at Fermi level  $\varepsilon_F$ .

The results of the modeling of thermopower

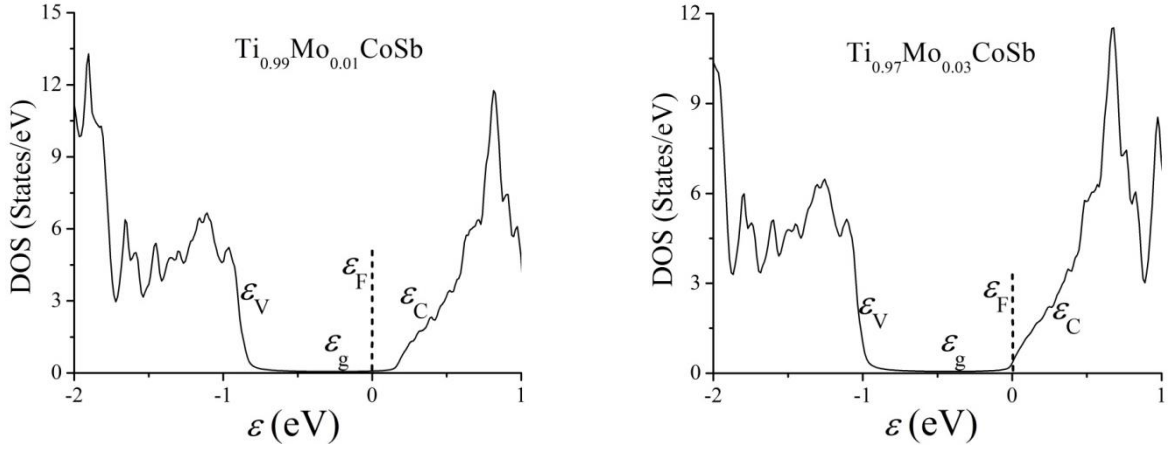


Fig. 2. Distribution of the electronic states density for ordered variant of the  $\text{Ti}_{1-x}\text{Mo}_x\text{CoSb}$  crystal structure.

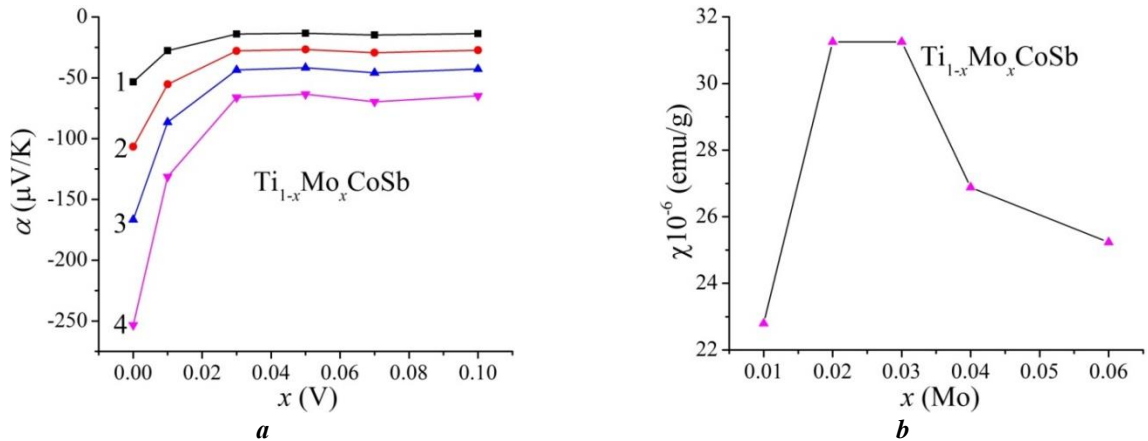


Fig. 3. Modeling of the thermopower coefficient behavior  $\alpha(x, T)$  (a) and variation of the magnetic susceptibility values  $\chi(x)$  (b) of  $\text{Ti}_{1-x}\text{Mo}_x\text{CoSb}$ .

coefficient  $\alpha(x, T)$  for  $\text{Ti}_{1-x}\text{Mo}_x\text{CoSb}$  show a sharp decrease in values with increasing of Mo impurity concentration. Under these conditions, negative values of  $\alpha(x)$  should be obtained in the experiment, and activation parts should disappear on the temperature dependences of electric resistivity  $\ln(\rho(1/T))$  of  $\text{Ti}_{1-x}\text{Mo}_x\text{CoSb}$  because the Fermi level  $\varepsilon_F$  and percolation level of conduction band  $\varepsilon_C$  should be crossed. The results of electrokinetic, energetic and magnetic studies of  $\text{Ti}_{1-x}\text{Mo}_x\text{CoSb}$  will show an agreement between performed calculations and actual processes in the semiconductor.

#### IV. Magnetic susceptibility study of $\text{Ti}_{1-x}\text{Mo}_x\text{CoSb}$

The results of magnetic susceptibility  $\chi(x)$  measurements of  $\text{Ti}_{1-x}\text{Mo}_x\text{CoSb}$  at 300 K are interesting (Fig. 3b). Performed studies showed that the  $\text{Ti}_{1-x}\text{Mo}_x\text{CoSb}$  samples are Pauli paramagnets, in which the  $\chi(x)$  values are determined by electron gas and are proportional to the density of states at the Fermi level  $g(\varepsilon_F)$ . As shown in Fig. 3b, the  $\chi(x)$  dependence in detail

repeats the character of structural changes, and, saying in advance, energetic parameters of  $\text{Ti}_{1-x}\text{Mo}_x\text{CoSb}$ .

At  $x > 0.01$ , the  $\chi(x)$  dependence rapidly changes the slope, reaches the plateau and does not change practically up to  $x = 0.03$ . Thus, the increase of impurity Mo concentration does not change practically the density of states values at the Fermi level  $g(\varepsilon_F)$ . Such  $\chi(x)$  behavior ( $\chi \sim g(\varepsilon_F)$ ) is only possible with appearance in  $\text{Ti}_{1-x}\text{Mo}_x\text{CoSb}$  current carriers of opposite sign which is a result of the generation of donor-acceptor pairs and cause invariability of density of states at the Fermi level  $g(\varepsilon_F)$ . At Mo atoms concentration  $x > 0.03$ , the electron concentration increases rapidly than holes, the Fermi level  $\varepsilon_F$  approaches the percolation level of the conduction band  $\varepsilon_C$ , that results in a decrease of the density of states at the Fermi level  $g(\varepsilon_F)$  for  $\text{Ti}_{1-x}\text{Mo}_x\text{CoSb}$ .

#### V. Electrokinetic and energetic characteristics study of $\text{Ti}_{1-x}\text{Mo}_x\text{CoSb}$

The temperature and concentration dependencies of

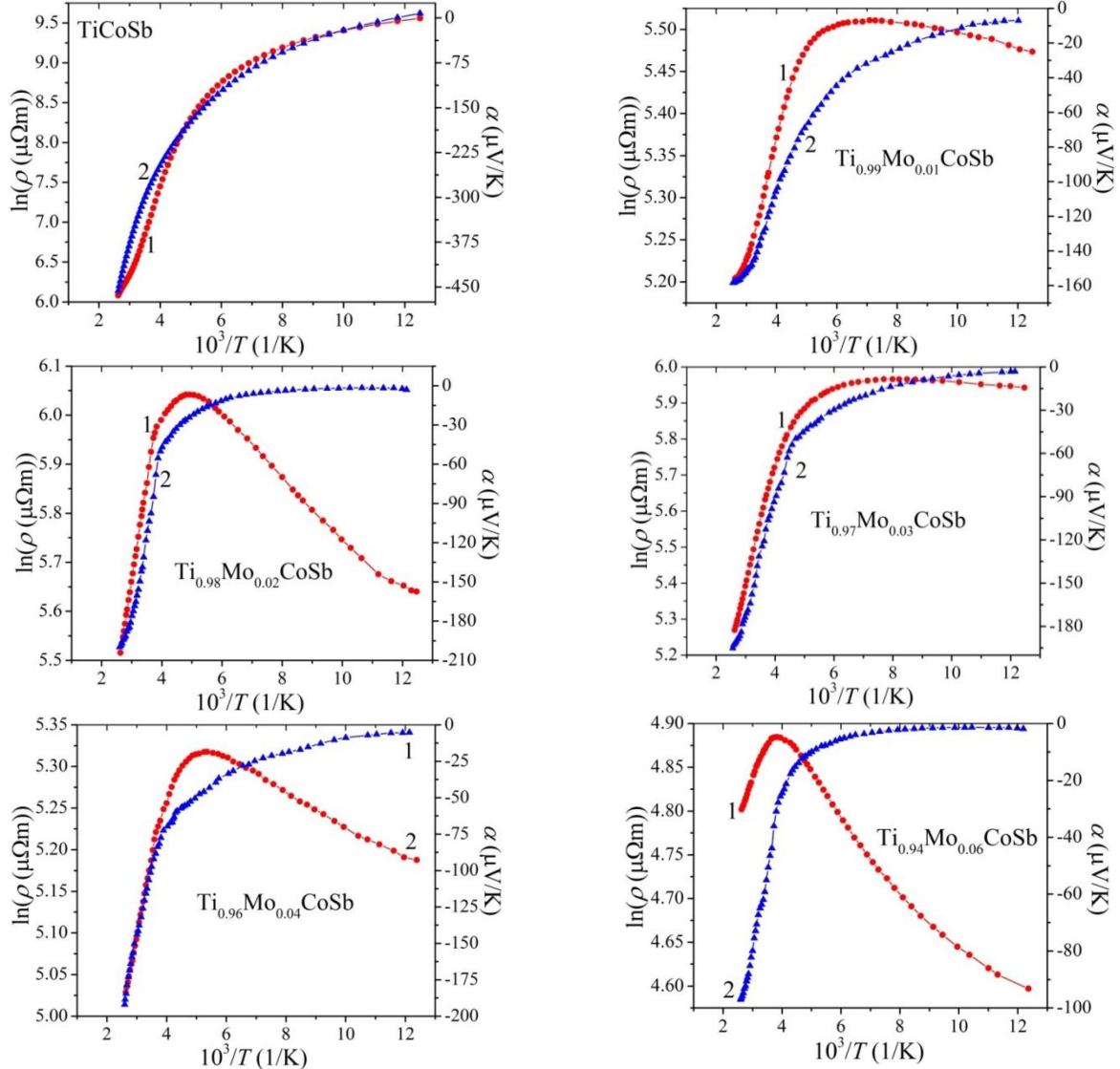


**Fig. 4.** Temperature dependencies of electric resistivity  $\ln(\rho(1/T))$  (1) and thermopower coefficient  $\alpha(1/T)$  (2) for  $\text{Ti}_{1-x}\text{Mo}_x\text{CoSb}$ .

### Investigation of $\text{Ti}_{1-x}\text{Mo}_x\text{CoSb}$ Semiconducting Solid Solution

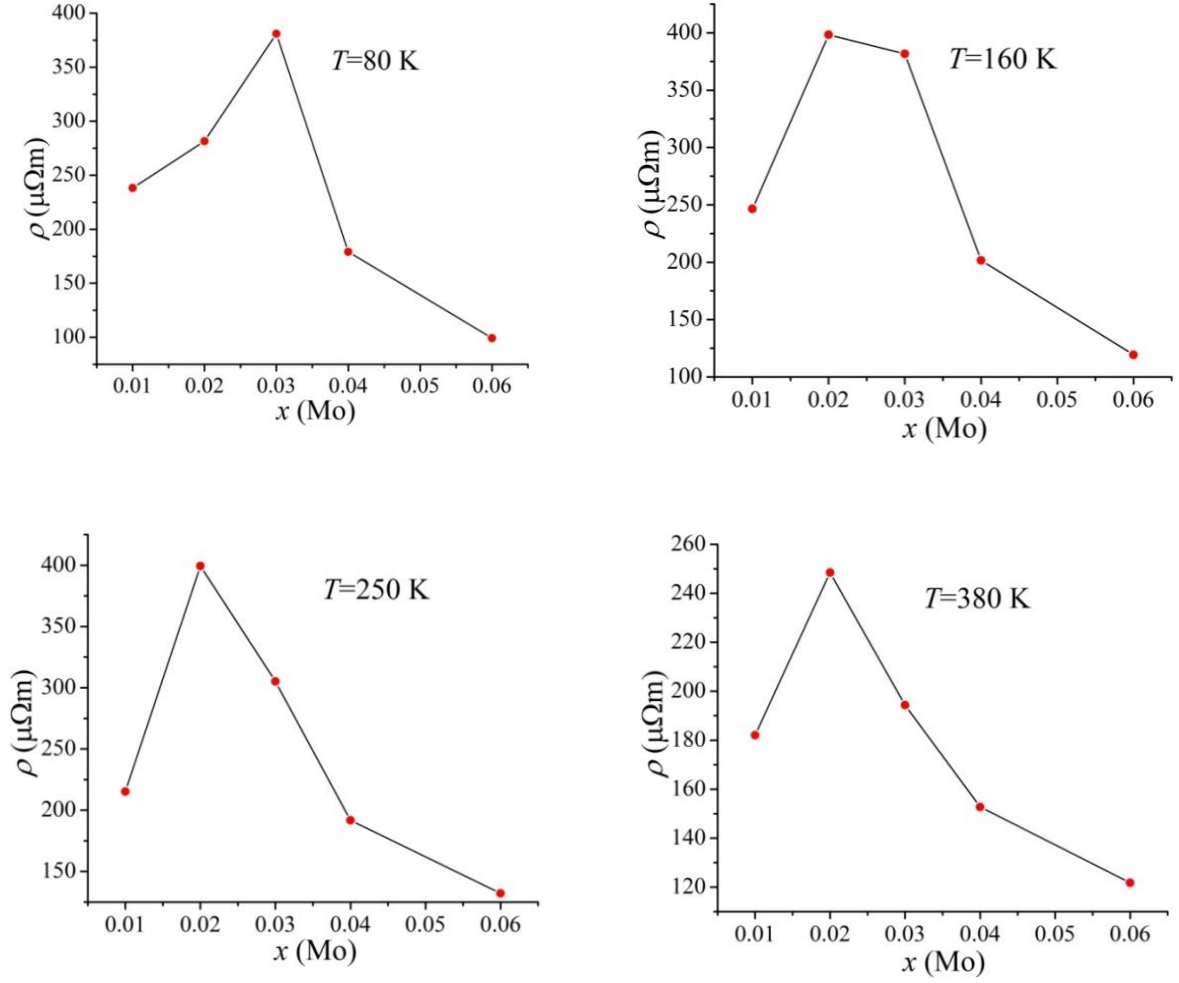


**Fig. 5.** Variation of electric resistivity values  $\rho(x,T)$  of  $\text{Ti}_{1-x}\text{Mo}_x\text{CoSb}$  at different temperatures.

the electric resistivity  $\rho(T,x)$  and the thermopower coefficient  $\alpha(T,x)$  of  $\text{Ti}_{1-x}\text{Mo}_x\text{CoSb}$  are shown in Figs. 4 - 6. Doping of the  $\text{TiCoSn}$  half-Heusler phase by Mo atoms changes the behavior of temperature and concentration dependencies of electric resistivity  $\rho(T,x)$  and thermopower coefficient  $\alpha(T,x)$  in the way that does not correspond to the results of modeling of the energetic characteristics of the semiconductor. Thus, electronic structure modeling showed that the substitution of Ti atoms by Mo atoms generates the structural defects of donor nature in  $\text{Ti}_{1-x}\text{Mo}_x\text{CoSb}$  with negative values of the thermopower coefficient  $\alpha(x,T)$ . Indeed, the thermopower coefficient  $\alpha(x,T)$  values of  $\text{Ti}_{1-x}\text{Mo}_x\text{CoSb}$  remain negative at all concentrations and temperatures. In addition, donor generation should result in an increase of free electrons number which causes decreasing of electric resistivity values  $\rho(x,T)$ .

Presence of the activation parts on  $\ln(\rho(1/T))$  dependencies at high temperatures for all studied  $\text{Ti}_{1-x}\text{Mo}_x\text{CoSb}$  samples was unexpected (Fig. 4). High-temperature activation of  $\ln(\rho(1/T))$  dependencies indicated the location of the Fermi level  $\varepsilon_F$  in the band gap  $\varepsilon_g$  of the semiconductor. On the other hand, the negative values of thermopower coefficient  $\alpha(x,T)$  for  $\text{Ti}_{1-x}\text{Mo}_x\text{CoSb}$  indicated that the Fermi level  $\varepsilon_F$  is located in the band gap near the conduction band  $\varepsilon_C$ .

The obtained result does not correspond to DOS

calculations of  $\text{Ti}_{1-x}\text{Mo}_x\text{CoSb}$  for the ordered variant of the structure in which Ti atoms in 4a position are substituted by Mo atoms that generates the structural defects of the donor nature. After all, according to performed calculations (Fig. 7), at concentration  $x \geq 0.03$ , the Fermi level  $\varepsilon_F$  and percolation level of conduction band will cross that result in the metallization of the conductivity.

The dependencies  $\ln\rho(1/T)$  and  $\alpha(1/T)$  of  $\text{Ti}_{1-x}\text{Mo}_x\text{CoSb}$  (Fig. 4) are typical for heavily doped and strongly compensated semiconductors (HDSCS) [12], and the presence of the activation parts indicate several mechanisms of charge transport. Such mechanisms are the activation of current carriers from the Fermi level  $\varepsilon_F$  to continuous energy bands (high temperatures) and hopping conduction over the energy states close to the Fermi level  $\varepsilon_F$  (low temperatures). The  $\ln\rho(1/T)$  dependencies of  $\text{Ti}_{1-x}\text{Mo}_x\text{CoSb}$  are described by known relation [12]:

$$\rho^{-1}(T) = \rho_1^{-1} \exp\left(-\frac{\varepsilon_1^\rho}{k_B T}\right) + \rho_3^{-1} \exp\left(-\frac{\varepsilon_3^\rho}{k_B T}\right), \quad (2)$$

where the first term at high temperatures describes the activation of current carriers  $\varepsilon_1^\rho$  from the Fermi level  $\varepsilon_F$  to the percolation levels of continuous energy band, and the second, low temperature, is the energy of hopping

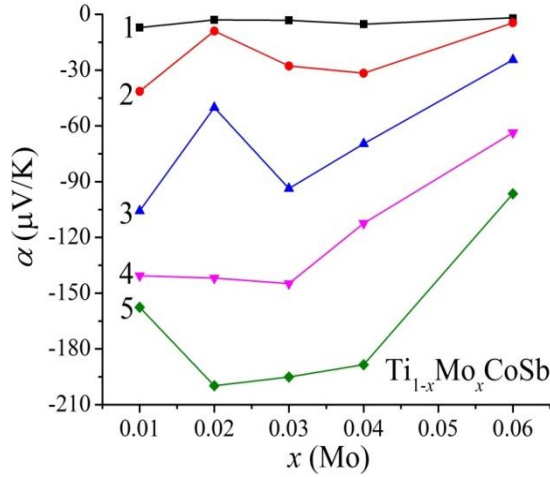


**Fig. 6.** Variation of thermopower coefficient values  $\alpha(x, T)$  of  $\text{Ti}_{1-x}\text{Mo}_x\text{CoSb}$  at different temperatures: 1 – 80 K, 2- 160 K, 3 – 250 K, 4 – 300 K, 5 – 380 K.

conduction  $\varepsilon_3^\rho$ .

The temperature dependences of the thermopower coefficient  $\alpha(1/T)$  for  $\text{Ti}_{1-x}\text{Mo}_x\text{CoSb}$  are described by relation [11]:

$$\alpha = \frac{k_B}{e} \left( \frac{\varepsilon_i^\alpha}{k_B T} - \gamma + 1 \right), \quad (3)$$

where  $\gamma$  is a parameter which depends on the scattering mechanisms. From the high-temperature parts of  $\alpha(1/T)$  dependencies the values of activation energy  $\varepsilon_1^\alpha$ , which are proportional to the large-scale fluctuation amplitude of the continuous energy band, were calculated. From the low-temperature parts of  $\alpha(1/T)$  dependencies the activation energy values  $\varepsilon_3^\alpha$ , which are proportional to the modulation amplitude of the small-scale fluctuation of HDSCS [12,13], were determined.

Doping of the  $\text{TiCoSb}$  compound by the lowest concentration of Mo atoms increases the values of electric resistivity  $\rho(x, T)$  for  $\text{Ti}_{1-x}\text{Mo}_x\text{CoSb}$  (Fig. 5) caused by the change of main current carriers concentration. In a semiconductor, this is possible due to the appearance of the high number of acceptors that capture free electrons and decrease their concentration in the conduction band  $\varepsilon_C$  (effect of “freezing” of electrons at acceptor levels [12]). In the case of the  $\text{Ti}_{1-x}\text{Mo}_x\text{CoSb}$  solid solution, the generation of structural defects of the acceptor nature is possible when the Mo atoms ( $4d^55s^1$ ) occupy the crystallographic position  $4c$  of Co atoms ( $3d^74s^2$ ) (Mo atom has less  $3d$ -electrons than Co).

Thus, the obtained experimental result allows to make important conclusion concerning structural peculiarities of  $\text{Ti}_{1-x}\text{Mo}_x\text{CoSb}$ : the introduction of Mo atoms in the  $\text{TiCoSb}$  structure does not lead to its ordering, and impurity atoms occupy simultaneously different crystallographic positions.

A change in values of electric resistivity  $\rho(x, T)$  for  $\text{Ti}_{1-x}\text{Mo}_x\text{CoSb}$  at different temperatures allows us to obtain information on the ratio of ionized donor and acceptor concentrations in the semiconductor. At 80 K, the maximum on  $\rho(x, T)$  dependence (Fig. 5) is reached at

Mo atom concentration,  $x \approx 0.03$ . At higher temperature ( $T = 250$  K) this maximum is blurred in concentration interval  $x = 0.02 \div 0.03$ . At even higher temperatures, it is located at a concentration  $x \approx 0.02$ .

This fact that the electric resistivity values  $\rho(x, T)$  of  $\text{Ti}_{1-x}\text{Mo}_x\text{CoSb}$  are higher at 160 K than at 80 K indicates that the number of current carriers has decreased. The decrease of electron concentration is not consistent with predicted donor generation, which supplies the electrons. On the one hand, this confirms the conclusion concerning simultaneous generation of donors and acceptors in  $\text{Ti}_{1-x}\text{Mo}_x\text{CoSb}$ , and on the other hand, it allows to state that the depth of location of impurity donor level (band) in the band gap  $\varepsilon_g$  of the semiconductor is greater than that of the acceptor level, and for donor ionization the higher temperatures are needed.

What does it mean?

It means that the  $\text{Ti}_{1-x}\text{Mo}_x\text{CoSb}$  semiconductor has at least two donor levels (bands): shallow  $\varepsilon_D^1$  and deep  $\varepsilon_D^2$ . At 80 K, the ionized states of the shallow donor level  $\varepsilon_D^1$  have created a certain number of free electrons in the conduction band. The maximum on the  $\rho(x, T)$  dependence at temperature  $T = 80$  K (Fig. 5) indicated that the concentrations of available in semiconductor ionized donors and acceptors are balanced (the number of places at the acceptor levels is slightly less than the number of free electrons). At 80 K, the impurity at Mo content  $x = 0.03$ , which generates acceptors, should be introduced to keep the hole and electron concentrations close. At higher temperatures, ionization of deep donors takes place, which increases their concentration, and maximum on  $\rho(x, T)$  dependence appears at lower Mo concentrations (maximum  $\rho(x, T)$  shifts to the left with temperature). Analysis of the structural characteristics of  $\text{Ti}_{1-x}\text{Mo}_x\text{CoSb}$  showed three possible variants of donor generation in the semiconductor: occupation of vacancies by Mo atoms in  $4a$  position, substitution of Ti atoms in this position or occupation of vacancies in  $4c$  position of Co atoms. The performed studies do not allow to establish a correspondence between nature of the structural donor defect and location depth of the impurity donor level (band) generated by it in the band gap  $\varepsilon_g$  of the  $\text{Ti}_{1-x}\text{Mo}_x\text{CoSb}$  semiconductor. For this, the next study will be devoted.

Thus, in the  $\text{Ti}_{1-x}\text{Mo}_x\text{CoSb}$  semiconductor, the concentration of ionized donors prevails the concentration of ionized acceptors and, quite logically, the total number of structural defects of the donor nature is higher than acceptor nature.

This conclusion was confirmed by the results of measurements of thermopower coefficient values  $\alpha(x, T)$  for  $\text{Ti}_{1-x}\text{Mo}_x\text{CoSb}$  at different concentrations and temperatures (Fig. 6). At 80 K the thermopower coefficient values  $\alpha(x, T)$  of  $\text{Ti}_{1-x}\text{Mo}_x\text{CoSb}$  change slightly: from  $\alpha(x = 0.01) = -7.1$   $\mu\text{V/K}$  up to  $\alpha(x = 0.03) = -3.1$   $\mu\text{V/K}$  and  $\alpha(x = 0.06) = -1.9$   $\mu\text{V/K}$ . Such behavior  $\alpha(x, T)$  shows that the  $\text{Ti}_{1-x}\text{Mo}_x\text{CoSb}$  semiconductor is strongly compensated at 80 K: a significant part of the free electrons, the source of which are shallow donors, are “frozen” on acceptors. With an increase of temperature the ionization of deeper donor levels (band) occurs, which enlarges electron concentration, and the  $\alpha(x, T)$  values increase.

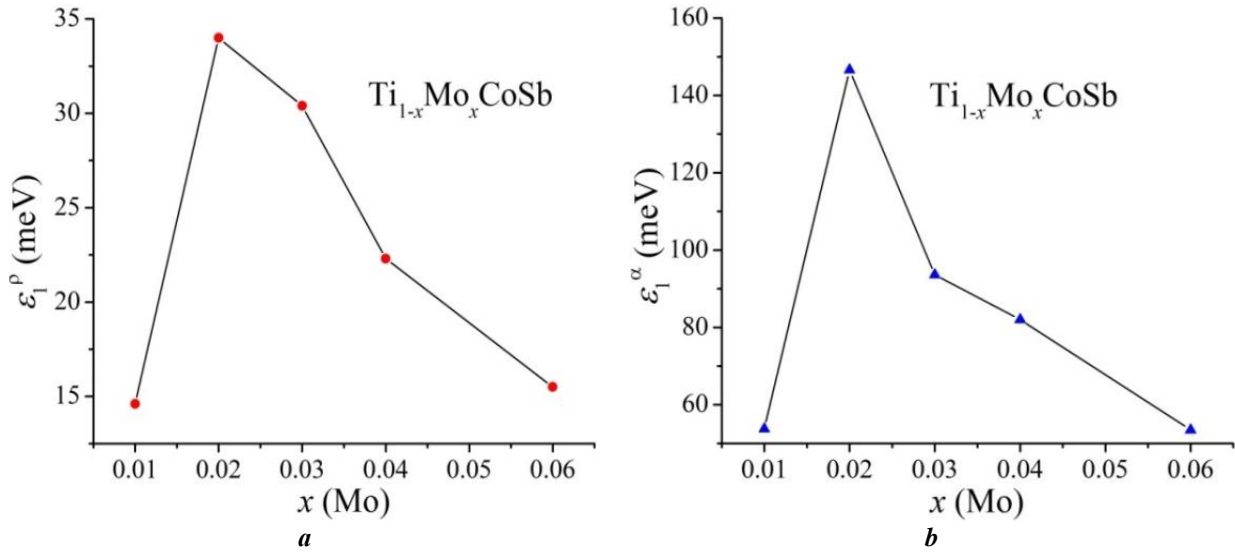


**Fig. 7.** Variation of the activation energy values  $\varepsilon_1^\rho(x)$  (a) and  $\varepsilon_1^\alpha(x)$  (b) for  $\text{Ti}_{1-x}\text{Mo}_x\text{CoSb}$ .

The presence of a maximum on the  $\alpha(x,T)$  dependence of  $\text{Ti}_{1-x}\text{Mo}_x\text{CoSb}$  at concentration  $x \approx 0.02$  in the temperature range  $160 \div 250$  K (Fig. 6, curves 2, 3) indicated a decrease of electron concentration at specified concentrations and temperatures due to their “freezing” on acceptors. At higher temperatures, when the deep impurity donor states of semiconductor are ionized, the concentration of free electrons significantly exceeds the number of acceptor levels in the band gap  $\varepsilon_g$  and maximum on  $\alpha(x,T)$  dependence of  $\text{Ti}_{1-x}\text{Mo}_x\text{CoSb}$  disappears.

The conclusion concerning simultaneous participation of electrons and holes in electrical conductivity of  $\text{Ti}_{1-x}\text{Mo}_x\text{CoSb}$  also follows from the analysis of energetic characteristics of the semiconductor. Since the temperature dependencies  $\ln(\rho(1/T))$  and  $\alpha(1/T)$  of  $\text{Ti}_{1-x}\text{Mo}_x\text{CoSb}$  are typical for doped and compensated semiconductors with available activation parts which indicate several mechanisms of charge transport, we can calculate their energetic parameters using known relations (2) and (3) [12,11]. From the activation parts of  $\ln(\rho(1/T))$  dependencies using equation (2), the activation energy of electrons  $\varepsilon_1^\rho$  from the Fermi level  $\varepsilon_F$  to the percolation level of the conduction band  $\varepsilon_C$  is calculated which allows, in particular, to determine the location of the Fermi level  $\varepsilon_F$  in the band gap  $\varepsilon_g$  of  $\text{Ti}_{1-x}\text{Mo}_x\text{CoSb}$  (Fig. 7a).

From the high- and low-temperature parts of the thermopower coefficient dependencies  $\alpha(1/T)$  based on relation (3) the activation energies  $\varepsilon_1^\alpha$  and  $\varepsilon_3^\alpha$  were calculated. The values  $\varepsilon_1^\alpha$  and  $\varepsilon_3^\alpha$  are proportional to the amplitude of modulation of continuous energy bands and the amplitude of small-scale fluctuation, respectively, of doped and compensated semiconductor (Fig. 7b).

The change of activation energy values  $\varepsilon_1^\rho$  from the Fermi level to the percolation level of conduction band showed that in the concentration range  $x = 0.01 \div 0.02$  the Fermi level  $\varepsilon_F$  moves away from the conduction band. At  $x = 0.01$  the depth of location of the Fermi level  $\varepsilon_F$  was  $\varepsilon_1^\rho(x = 0.01) = 14.6$  meV, and at a higher concentration

of Mo atoms ( $x = 0.02$ ) the Fermi level  $\varepsilon_F$  “runs away” from the conduction band  $\varepsilon_C$  at the distance  $\varepsilon_1^\rho(x = 0.02) = 34.1$  meV. It is possible when acceptor impurity is introduced in the semiconductor of electron type of conductivity, which decreases the free electron concentration lowering the position of the Fermi level  $\varepsilon_F$  relative to the bottom of the conduction band  $\varepsilon_C$ . As noted above, for  $\text{Ti}_{1-x}\text{Mo}_x\text{CoSb}$  it is possible only in the case when Co atoms in position 4c are substituted by Mo atoms.

However, at concentration  $x = 0.03$  the Fermi level  $\varepsilon_F$  returns its motion and again approaches to the percolation level of the conduction band  $\varepsilon_C$  at the distance  $\varepsilon_1^\rho(x = 0.03) = 30.4$  meV. Thus, in the concentration range  $x = 0.01 \div 0.02$ , the rate of generation of structural defects of acceptor nature prevails the rate of the donor generation. And only at concentrations  $x \geq 0.03$  the rate of increase of donor concentration is higher than the rate of acceptor increase. At subsequent Mo atom concentrations, the Fermi level  $\varepsilon_F$  moves to the conduction band  $\varepsilon_C$  and at concentration  $x = 0.06$  approaches its percolation level at the distance  $\varepsilon_1^\rho(x = 0.06) = 15.5$  meV.

This conclusion also follows from the character variation of activation energy value  $\varepsilon_1^\alpha(x)$ , which is proportional to modulation amplitude of continuous energy band of  $\text{Ti}_{1-x}\text{Mo}_x\text{CoSb}$  (Fig. 7b) and represents compensation degree of semiconductor [12]. After all, simultaneous generation in the crystal of structural defects of the donor and acceptor nature is accompanied by variation of the compensation degree and variation of modulation amplitude of continuous energy band HDSCS [1, 9] by the law which represents the relation of ionized donors and acceptors. As shown in Fig. 7b, in the concentration range  $x = 0.01 \div 0.02$  the modulation amplitude value increases from  $\varepsilon_1^\alpha(x = 0.01) = 53.8$  meV and reaches maximum at  $x = 0.02$   $\varepsilon_1^\alpha(x = 0.02) = 146.6$  meV. Thus, at a concentration  $x = 0.02$ , the state of the highest compensation is achieved: the concentrations of ionized donors and

acceptors are as close as possible.

At higher impurity Mo atom concentration the modulation amplitude of continuous energy band of  $Ti_{1-x}Mo_xCoSb$  decreases from  $\varepsilon_1^\alpha(x=0.03) = 93.6$  meV to  $\varepsilon_1^\alpha(x=0.06) = 53.5$  meV, indicating that the compensation degree of semiconductor decreases because of the higher rate of the donor generation than acceptors.

## Conclusions

Thus, the results of the structural, electrokinetic, energetic and magnetic studies of the  $Ti_{1-x}Mo_xCoSb$  semiconducting solid solution allow saying about the complicated mechanism of simultaneous generation structural defects of the acceptor and donor nature (donor-acceptor pairs) in the crystal. It should be noted, that the structural studies of  $Ti_{1-x}Mo_xCoSb$  did not find such defects, because their concentration is beyond the accuracy of the X-ray method investigation. It is

important to understand the mechanism of simultaneous generation of the structural defects of the acceptor and donor nature (donor-acceptor pairs), i.e. what changes in all crystallographic positions of the unit cell of the  $Ti_{1-x}Mo_xCoSb$  solid solution occur. This question requires further investigations and calculations of electronic state density distribution for all variants of atom distribution in  $Ti_{1-x}Mo_xCoSb$ . The calculated structure model, the behavior of the energetic characteristics of which will correspond to the experimental results, will be maximal close to the real structure of the crystal.

**Stadnyk Yu.** - Ph.D., Senior Scientist;  
**Romaka V.** – Professor;  
**Horyn A.** - Ph.D., Senior Research;  
**Romaka L.** - Ph.D., Senior Scientist;  
**Krayovskyy V.** - associate professor, Ph.D;  
**Romaniv I.** -Ph.D. student;  
**Rokomanuk M.** - Ph.D. student.

- [1] V.A. Romaka, M.G. Shelyapina, Yu.V. Stadnyk, D. Frushart, L.P. Romaka, V.F. Chekurin, *Semiconductors*, 40 (№7), 776 (2006) (<https://doi.org/10.1134/S1063782606070074>).
- [2] L.P. Romaka, M.G. Shelyapina, Yu.V. Stadnyk, D. Fruchart, E.K. Hlil, V.A. Romaka, *J. Alloys Compd.* 416, 46 (2006) (<https://doi.org/10.1016/j.jallcom.2005.08.051>).
- [3] Yu. Stadnyk, V.A. Romaka, M. Shelyapina, Yu. Gorelenko, L. Romaka, D. Fruchart, A. Tkachuk, V. Chekurin, *J. Alloys Compd.*, 421, 19 (2006) (<https://doi.org/10.1016/j.jallcom.2005.11.008>).
- [4] V.A. Romaka, Yu.V. Stadnyk, L.G. Akselrud, V.V. Romaka, D. Frushart, P. Rogl, V.N. Davydov, Yu.K. Gorelenko, *Semiconductors*, 42 (№7), 753 (2008) (<https://doi.org/10.1134/S1063782608070014>).
- [5] V.A. Romaka, Yu.V. Stadnyk, P. Rogl, L.G. Akselrud, V.M. Davydov, V.V. Romaka, Yu.K. Gorelenko, A.M. Horyn, *Ukr. J. Phys.*, 53 (№2), 158 (2008).
- [6] V.A. Romaka, Yu.V. Stadnyk, P. Rogl, D. Fruchart, Yu.K. Gorelenko, L.P. Romaka, A.M. Horyn, *Ukr. J. Phys.*, 53 (№9), 889 (2008).
- [7] T. Roisnel, J. Rodriguez-Carvajal, *Mater. Sci. Forum*, Proc. EPDIC7, 378-381, 118 (2001) (<https://doi.org/10.4028/www.scientific.net/MSF.378-381.118>).
- [8] M. Schrueter, H. Ebert, H. Akai, P. Entel, E. Hoffmann, G.G. Reddy, *Phys. Rev. B* 52, 188 (1995) (<https://doi.org/10.1103/PhysRevB.52.188>).
- [9] V.L. Moruzzi, J.F. Janak, A.R. Williams, *Calculated electronic properties of metals*, Pergamon Press, NY, 1978.
- [10] V.V. Romaka, L.P. Romaka, V.Ya. Krayovskyy, Yu.V. Stadnyk, *Studies of rare earth and transition metals*, L'vivska Politekhnika, Lviv, 2015. [in Ukrainian].
- [11] B. I. Shklovskii and A. L. Efros, *Electronic Properties of Doped Semiconductors*, Springer, NY, 1984.
- [12] N.F. Mott and E.A. Davis, *Electron Processes In Non-crystalline Materials*, Clarendon Press, Oxford, 1979.

Ю. Стадник<sup>1</sup>, В.А. Ромака<sup>2</sup>, А. Горинь<sup>1</sup>, Л. Ромака<sup>1</sup>, В. Крайовський<sup>2</sup>,  
І. Романів<sup>1</sup>, М. Рокоманюк<sup>2</sup>

## Дослідження напівпровідникового твердого розчину $Ti_{1-x}Mo_xCoSb$

<sup>1</sup>Львівський національний університет ім. І.Франка, Львів, Україна, e-mail: stadnyku@gmail.com

<sup>2</sup>Національний університет "Львівська політехніка", Львів, Україна, vromaka@lp.edu.ua

Досліджено вплив легування сполуки  $TiCoSb$  (структурний тип  $MgAgAs$ ) атомами  $Mo$  на особливості структурних характеристик та поведінку кінетичних, енергетичних та магнітних властивостей напівпровідникового твердого розчину  $Ti_{1-x}Mo_xCoSb$  ( $x = 0 - 0,06$ ) в інтервалі температур 80 - 400 К. Показано, що уведення атомів  $Mo$  ( $r_{Mo} = 0,140$  нм) до структури сполуки  $TiCoSb$  шляхом заміщення у позиції  $4a$  атомів  $Ti$  ( $r_{Ti} = 0,146$  нм) супроводжується немонотонною зміною значень періоду елементарної комірки  $a(x)$ , вказуючи на непрогнозовані структурні зміни. На основі аналізу зміни значень питомого опору, коефіцієнта термо-ерс, магнітної сприйнятливості та енергетичних характеристик зроблено висновок про одночасне генерування у кристалі структурних дефектів донорної та акцепторної природи (донорно-акцепторні пари), які породжують відповідні енергетичні рівні у забороненій зоні напівпровідника та визначають його електропровідність.

**Ключові слова:** твердий розчин, електропровідність, коефіцієнт термо-ерс, рівень Фермі.